Journal of Power Sources 261 (2014) 148–155

Contents lists available at ScienceDirect

Journal of Power Sources

journal homepage: www.elsevier.com/locate/jpowsour

Enhanced cyclability of $LiNi_{0.5}Mn_{1.5}O_4$ cathode in carbonate based electrolyte with incorporation of tris(trimethylsilyl)phosphate (TMSP)

Haibo Rong [a], Mengqing Xu [a,b,c,*], Lidan Xing [a,b,c], Weishan Li [a,b,c,*]

[a] School of Chemistry and Environment, South China Normal University, Guangzhou 510006, China
[b] Key Laboratory of Electrochemical Technology on Energy Storage and Power Generation of Guangdong Higher Education Institutes, South China Normal University, Guangzhou 510006, China
[c] Engineering Research Center of Materials and Technology for Electrochemical Energy Storage, Ministry of Education, South China Normal University, Guangzhou 510006, China

HIGHLIGHTS

- TMSP is used as an electrolyte additive for $LiNi_{0.5}Mn_{1.5}O_4$ cathode battery at high voltage (4.9 V).
- The cyclability of the Li-ion battery at RT and ET can be improved by the use of TMSP.
- The rate capability of the Li-ion battery can be improved by the use of TMSP.
- Incorporation of TMSP can form a more stable and more conductive surface film on the cathode.

ARTICLE INFO

Article history:
Received 25 December 2013
Received in revised form
20 February 2014
Accepted 12 March 2014
Available online 21 March 2014

Keywords:
Lithium ion battery
Tris(trimethylsilyl)phosphate
Electrolyte additive
$LiNi_{0.5}Mn_{1.5}O_4$ cathode
High voltage
Cyclability

ABSTRACT

In this work, tris (trimethylsilyl) phosphate (TMSP) is used as an electrolyte additive to improve the cycling performance of $Li/LiNi_{0.5}Mn_{1.5}O_4$ cell upon cycling at high voltage, 4.9 V vs. Li/Li^+ at room temperature and elevated temperature (55 °C). The effects of TMSP on the cathode interface and the cycling performance of $Li/LiNi_{0.5}Mn_{1.5}O_4$ cell were investigated via the combination of electrochemical methods, including cycling test, cyclic voltammetry (CV), chronoamperometry, and electrochemical impedance spectroscopy (EIS). It is found that cells with electrolyte containing TMSP have better capacity retention than that of the cells without TMSP upon cycling at high voltage at room temperature and elevated temperature. The functional mechanism of incorporation of TMSP to the electrolyte to improve the cycling performance is conducted with ex-situ analysis approaches, including X-ray diffraction (XRD), scanning electron microscope (SEM), thermal gravimetric analysis (TGA), X-ray photoelectron spectroscopy (XPS), transmission electron microscope (TEM) and ICP-MS. The surface analysis results reveal that more stable and more conductive surface layer is formed on the $LiNi_{0.5}Mn_{1.5}O_4$ electrode with TMSP containing electrolyte, which is a leading factor for the enhanced the cycling performance of $Li/LiNi_{0.5}Mn_{1.5}O_4$ cells upon cycling at high voltage at room temperature and elevated temperature.

1. Introduction

In order to satisfy the requirements of higher energy density of Li-ion batteries for electric vehicles (EVs) and hybrid electric vehicles (HEVs), cathode materials with high operating potentials (>4.5 V, vs. Li/Li^+) have been extensively pursued in current Li-ion battery community [1]. $LiNi_{0.5}Mn_{1.5}O_4$ is one of the promising cathode materials for high energy density of Li-ion battery [2] because of its high operating voltage (4.75 vs. Li/Li^+), and high specific capacity (146.7 mAh g^{-1}) as well [3]. However, it is difficult to maintain the cycling stability of $LiNi_{0.5}Mn_{1.5}O_4$ in $LiPF_6$/carbonate based electrolyte at high voltage [4–6], which can be ascribed to the two possible reasons. The first of which is that the instability of the conventional electrolyte on the high charged cathode electrode (>4.5 V, vs. Li/Li^+), which causes severer decomposition of electrolyte and continuous growth of surface layer, leading to low coulombic efficiency, fast capacity loss, and huge gas generation [7,8]. The second reason is that the dissolution of Mn or Ni upon cycling at high voltage due to the disproportionation reaction occurring, $2Mn^{3+} = Mn^{4+} + Mn^{2+}$. The soluble Mn^{2+} migrates to

* Corresponding authors. School of Chemistry and Environment, South China Normal University, Guangzhou 510006, China. Tel./fax: +86 20 39310256.
E-mail addresses: mqxu@scnu.edu.cn, xumq5510@gmail.com (M. Xu), liwsh@scnu.edu.cn (W. Li).

http://dx.doi.org/10.1016/j.jpowsour.2014.03.032
0378-7753/

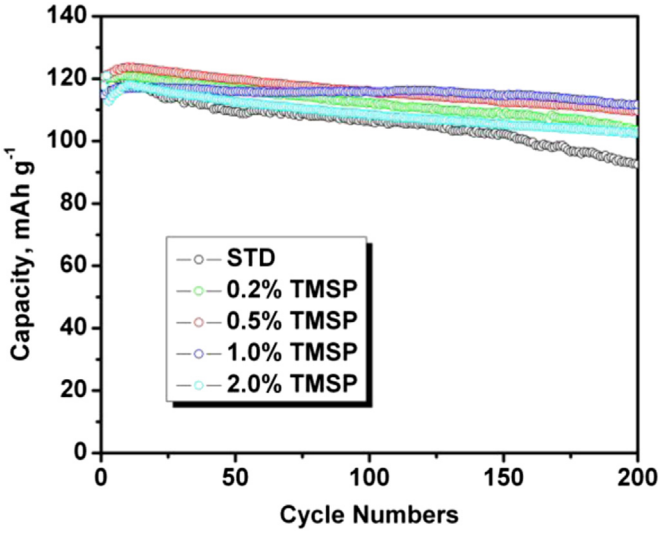

Fig. 1. Cycling performances profiles of Li/$LiNi_{0.5}Mn_{1.5}O_4$ cells using blank electrolyte (STD), 0.2, 0.5, 1.0 and 2.0 wt.% TMSP-containing electrolyte.

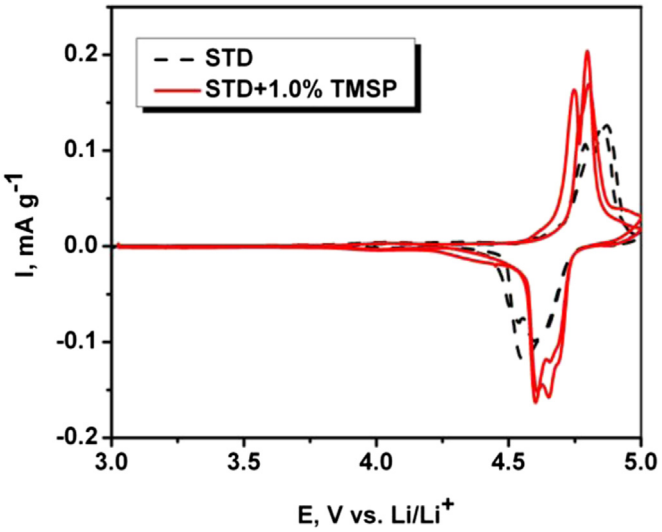

Fig. 3. Cyclic voltammetry profiles of $LiNi_{0.5}Mn_{1.5}O_4$ electrode in STD and TMSP containing electrolyte.

the anode surface and being reduced to Mn (0) during the charging process, which subsequently disrupts the SEI on anode surface, leading to dissolution/reformation of SEI on the anode electrode [9]. The dissolution/reformation of SEI process involves additional Li^+ loss and capacity fading upon cycling.

Various methods have been addressed to solve the above problems. Modification of the $LiNi_{0.5}Mn_{1.5}O_4$ material is generally proceed by doping with highly elecrto-negative ions or surface coating with various inorganic oxides [10], such as Bi_2O_3 [11], ZnO [12,13], ZrO_2 [14], ZrP_2O_7 [14], but the procedures always involve high cost and may be difficult to scale up for commercial applications [3]. Using novel solvents to replace the conventional carbonates has also been reported, such as lactone [15] and sulfone [16,17] due to its high stability at high voltage, but its high viscosity and unfavorable forming of SEI on graphite limits its application.

The use of electrolyte additives is one of the most economic and effective methods for the improvement of Li-ion battery performance [18]. Dalavi et al. reported Lithium bis (oxalato) borate (LiBOB) as an additive to improve the performance of Li/$LiNi_{0.5}Mn_{1.5}O_4$ cell [19]. The Li/$LiNi_{0.5}Mn_{1.5}O_4$ cell with 1.0 M $LiPF_6$ in EC/DEC (1/2, v/v) with 0.25% LiBOB exhibited better cycling capacity retention than the cells containing the standard electrolyte. Xu et al. reported Tris (pentafluorophenyl) phosphine (TPFPP) as an electrolyte additive to improve the cycling performance of Li/$LiNi_{0.5}Mn_{1.5}O_4$ cell [20]. With the incorporation of 0.5% TPFPP to 1.0 M $LiPF_6$ in EC/DMC/DEC (1/1/1, v/v) solution, the cycling stability has been significantly improved. Zhang et al. reported that Li/Li$[Li_{0.2}Ni_{0.13}Mn_{0.54}Co_{0.13}]O_2$ cells with addition of 1.0% (trimethylsilyl) phosphate (TMSP) present more excellent cycling performance than that without TMSP [21]. Yan et al. reported tris (trimethylsilyl) phosphate (TMSP) as a film-forming additive for Li/$LiNi_{0.5}Co_{0.2}Mn_{0.3}O_2$ cells, with addition of 1.0% TMSP to 1.0 M $LiPF_6$ in EC/EMC (3/7, in wt.%) solution, the cyclability was enhanced obviously [22]. However, the use of TMSP additive for high voltage spinel $LiNi_{0.5}Mn_{1.5}O_4$ cathode has not been reported yet.

In this work, tris (trimethylsilyl) phosphate (TMSP) was considered as an additive to improve the cyclability of Li/$LiNi_{0.5}Mn_{1.5}O_4$ cells at 4.9 V upon cycling at room temperature and elevated temperature (55 °C). Electrochemical methods and ex-situ

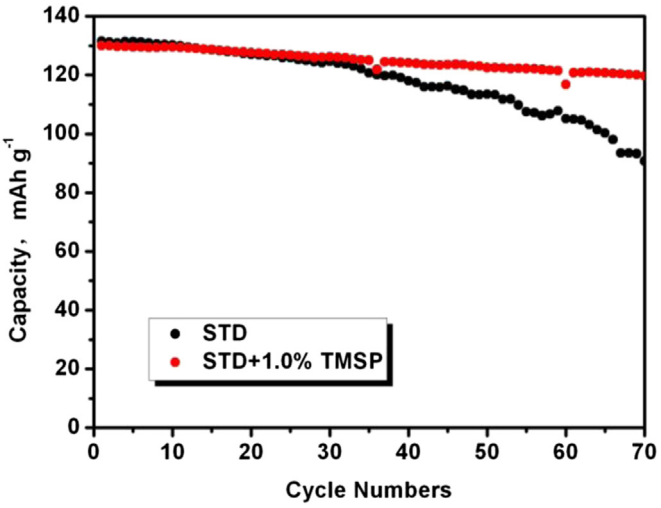

Fig. 2. Cycling performances of Li/$LiNi_{0.5}Mn_{1.5}O_4$ cells with and without TMSP containing at 55 °C.

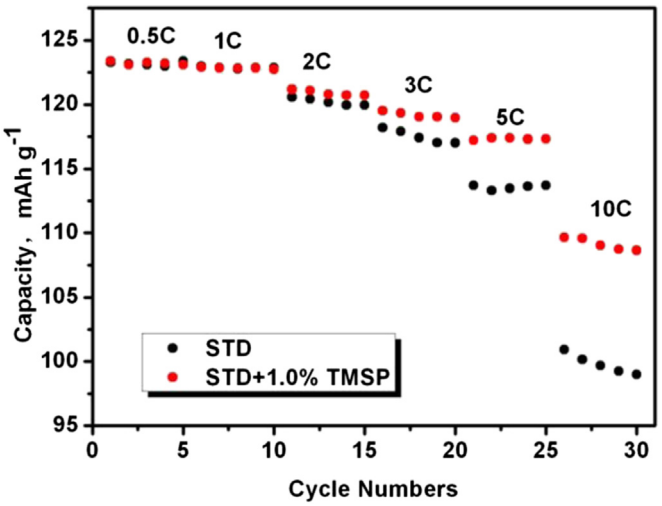

Fig. 4. Rate performances of Li/$LiNi_{0.5}Mn_{1.5}O_4$ cells with and without TMSP containing.

analysis have been employed to understand the role of TMSP in the enhanced performance of Li/$LiNi_{0.5}Mn_{1.5}O_4$ cells.

2. Experimental section

2.1. Preparation

Battery-grade carbonate solvents and lithium hexafluorophosphate ($LiPF_6$) were provided by Guangzhou Tinci Materials Technology Co. Ltd, China, and used without further purification. Tris (trimethylsilyl) phosphate (TMSP) was purchased from Fujian Chuangxin Technology Co. Ltd, China (>99.5%) and used without further purification. The blank electrolyte (STD) with a general composition is 1.0 M $LiPF_6$ in EC/DMC (1/2, v/v) solution, and the electrolytes with various contents of TMSP (0.2, 0.5, 1.0 and 2.0 wt.%) in the above blank electrolyte were prepared in a high purify argon-filled glove box (MBraun, Germany). The contents of water and free acid (HF) in the electrolyte was controlled below 20 and 50 ppm, respectively, which determined by Karl-Fisher 831 Coulometer (Metrohm, Switzerland) for H_2O and Karls-Fisher 798 GPT Titrino (Metrohm, Switzerland) for HF. The cathode electrode was prepared with the mixture of 80 wt.% $LiNi_{0.5}Mn_{1.5}O_4$, which was provided by Sichuan Xingneng Co. Ltd, China, 10 wt.% polyvinylidene fluoride (PVDF) binder, 5 wt.% acetylene black and 5 wt.% Super-P in *N*-methyl-pyrrolidone (NMP). The mixture slurry was coated on Al foil and dried at 85 °C for 2 h, then dried at 120 °C for 6 h under vacuum. The Li/$LiN_{0.5}Mn_{1.5}O_4$ cells were assembled with 2025-coin type using Celgard 2400 as separator in the argon-filled glove box, in which the water and oxygen content were less than 0.1 ppm.

2.2. Electrochemical measurements

Electrochemical behaviors of $LiN_{i0.5}Mn_{1.5}O_4$ electrodes in STD and TMSP containing electrolyte were determined by cyclic voltammetry (CV), with scan rate of 0.05 mV s^{-1}, and chronoamperometry on Solartron-1470 instrument (England). The cycling performance of the cells was evaluated on LAND system (CT2001A, China), and the cells were cycled at room temperature (25 °C) and elevated temperature (55 °C). Rate performances of the cells with and without TMSP were conducted on Arbin (BT2000),

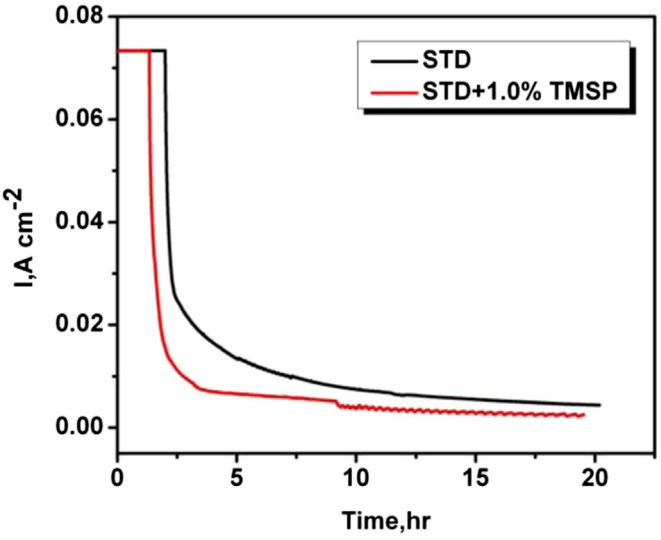

Fig. 5. Chronoamperometric responses profiles of Li/$LiNi_{0.5}Mn_{1.5}O_4$ cells in STD and TMSP containing electrolyte.

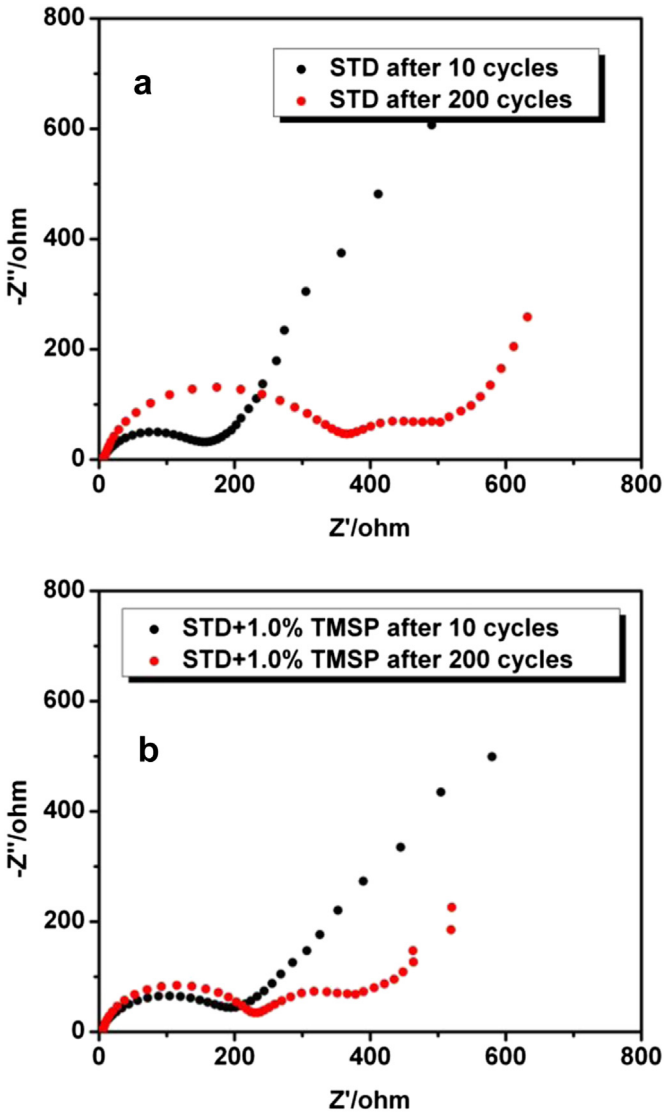

Fig. 6. Electrochemical impedance spectra patterns of Li/$LiNi_{0.5}Mn_{1.5}O_4$ cells without (a) and with TMSP (b).

with the current of 0.5 C, 1 C, 2 C, 3 C, 5 C, and 10 C. Cells were cycled according to the following protocol: the cells were charged to 4.9 V at a constant current (CC mode) followed by a constant-voltage charge ($V = 4.9$ V, CV mode) until the current decreased to 10% of applied charging current, and then the cells were discharged to 3.0 V with the same constant current (CC mode). Electrochemical impedance spectra (EIS) measurements were performed on a PGSTAT-30 electrochemical station (Autolab Metrohm, Nether lands) in a frequency range of 10^5–0.01 Hz with an amplitude of 5 mV.

The $LiNi_{0.5}Mn_{1.5}O_4$ electrodes and lithium foils after cycling were rinsed with anhydrous DMC three times to remove residual EC and $LiPF_6$ salt precipitated on the surface, and then evacuated overnight at room temperature before ex-situ analysis. The electrodes were exposed to air for less than 1 min during the sample-introduction process, which does not change the surface morphology and composition. To better understand the changes of crystal structure and the morphology of the $LiNi_{0.5}Mn_{1.5}O_4$ electrodes before and after cycling, XRD analysis and SEM observation were employed to investigate the changes. XRD was conducted on a XRD (Bruker D8 Advance, Germany) by scanning in the 2θ range of

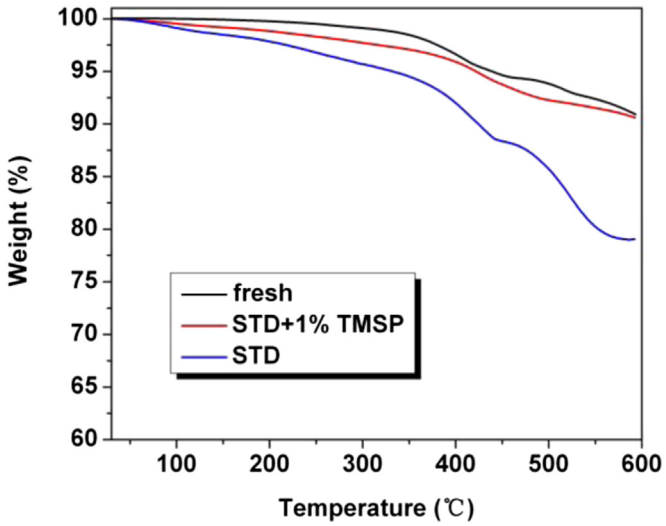

Fig. 7. TGA profiles of the fresh and cycled $LiNi_{0.5}Mn_{1.5}O_4$ electrodes with and without TMSP.

10–80°, and SEM was performed on JSM-6510, Japan, respectively. Thermal behaviors of the electrodes were analyzed on a TGA (TGA7, USA) instrument with temperature ramping from room temperature to 600 °C. The contents of Mn and Ni deposited on Li foils were determined by ICP-MS (IRIS Intrepid II XSP, USA). Transmission electron microscope (TEM) (JEM-2100HR, Japan) was used to study the film on the $LiNi_{0.5}Mn_{1.5}O_4$ electrodes. The XPS spectra were carried out with (ESCALAB 250, USA) to analyze the chemical composition of the surface of the $LiNi_{0.5}Mn_{1.5}O_4$ electrodes. Calibration of XPS peak position was made by recording XPS spectra for reference compounds, which are present on the electrode surface: LiF, PVDF, and $Li_xPO_yF_z$. The universal contamination of C–H bond at 284.8 eV was used as a reference for the final adjustment of the energy scale in the spectra. Elemental concentration was calculated based on the equation: $C_x = (I_x/S_x)/(\sum I_x/S_x)$, where I_x is the relative intensity of the element, and S_x is the sensitivity value of the element.

3. Results and discussion

Fig. 1 shows the cycling performance of $Li/LiNi_{0.5}Mn_{1.5}O_4$ cells at room temperature and 4.9 V, vs. Li/Li^+. It can be observed that cells with TMSP containing electrolyte have better cycling performance than that without TMSP at room temperature (25 °C). The cell without TMSP presents a distinct capacity fade from 120.7 mAh g^{-1} down to 92.5 mAh g^{-1} with a capacity retention of 76.6% after 200 cycles. However, the capacity retention of the cells with 0.2, 0.5, 1.0 and 2.0 wt.% TMSP containing electrolyte is 85.5%, 88.6%, 95.4% and 84.2%, respectively. This suggests that the incorporation of TMSP can significantly improve the cycling stability, and the cell with 1.0 wt.% TMSP containing electrolyte has superior cycling performance than that of other concentrations of TMSP added. The cycling performance of $Li/LiNi_{0.5}Mn_{1.5}O_4$ cells at elevated temperature (55 °C) was shown in Fig. 2, cell with addition of 1.0% TMSP has superior cyclability than the baseline electrolyte with a capacity retention of 94.9% after 70 cycles at elevated temperature, while it is only 70% for the cells with baseline electrolyte. This also indicates that the use of 1.0% TMSP can enhance the cycling stability of $Li/LiNi_{0.5}Mn_{1.5}O_4$ cells at both high voltage and elevated temperature.

Cyclic voltammetry was employed to better understand the electrochemical behaviors of $LiNi_{0.5}Mn_{1.5}O_4$ electrode in the electrolyte with and without TMSP added. Fig. 3 shows the cyclic voltammetry profiles of the $LiNi_{0.5}Mn_{1.5}O_4$ electrode in the electrolyte with and without TMSP added. Upon the anodic sweep, the $LiNi_{0.5}Mn_{1.5}O_4$ electrode in baseline (STD) electrolyte shows three typical oxidation peaks, occurring at 4.0, 4.7, and 4.8 V, which are corresponding to extracting/removal of lithium ions from cathode material and accordingly to the oxidation of transition metals, Mn^{3+}/Mn^{4+}, and Ni^{2+}/Ni^{3+}, Ni^{3+}/Ni^{4+}, respectively [23]. During the cathodic scan, the two intercalation/insertion processes of lithium ions into cathode material merged, showing only sole reduction peak at around 4.6 V. As regards to the $LiNi_{0.5}Mn_{1.5}O_4$

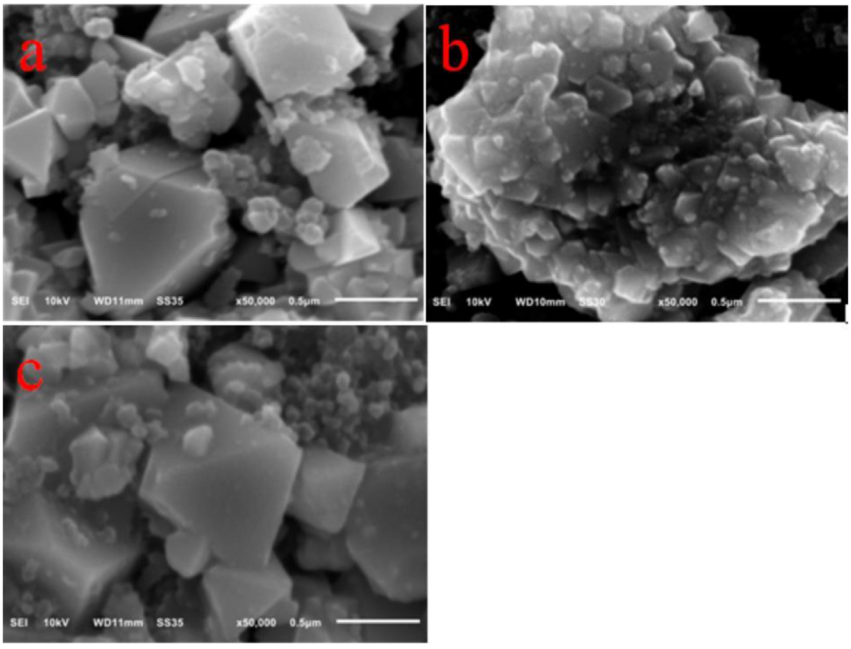

Fig. 8. SEM images of the fresh (a) and cycled $LiNi_{0.5}Mn_{1.5}O_4$ electrodes without (b) and with TMSP (c).

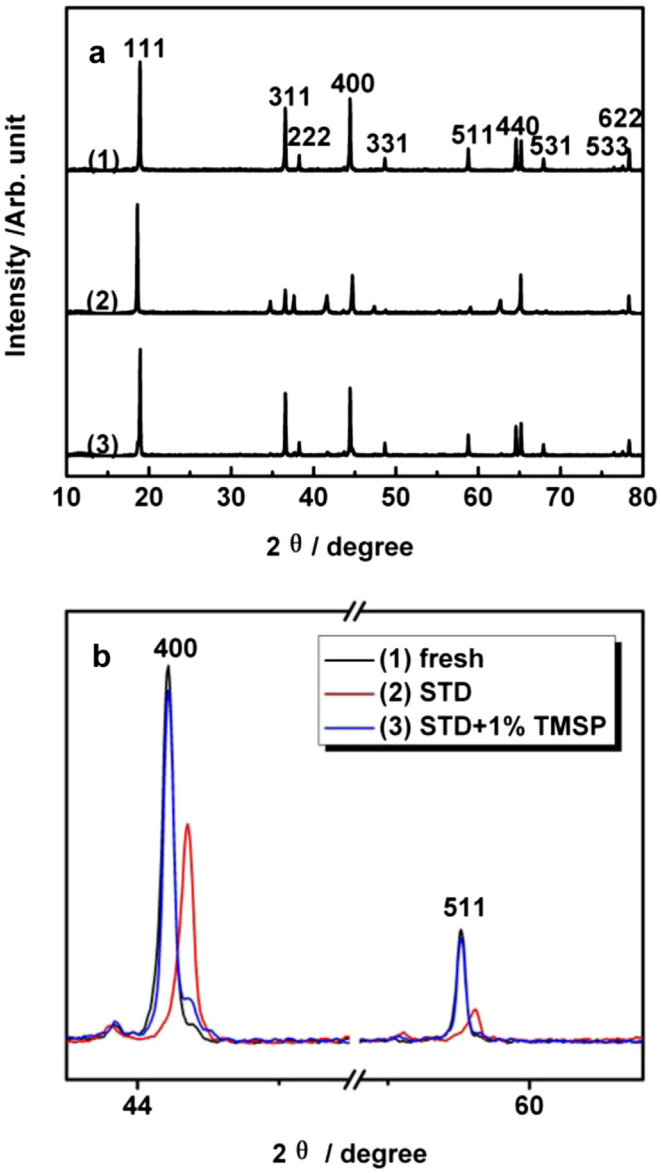

Fig. 9. XRD patterns of the fresh (1) and cycled $LiNi_{0.5}Mn_{1.5}O_4$ electrodes without (2) and with TMSP (3).

electrode in the electrolyte with 1.0% TMSP containing electrolyte, different electrochemical behavior was observed upon the anodic/cathodic scans. The redox current of the $LiNi_{0.5}Mn_{1.5}O_4$ in TMSP containing electrolyte is higher than that of baseline, suggesting faster kinetics of lithium ions removal/insertion from/into the $LiNi_{0.5}Mn_{1.5}O_4$ electrode is achieved by the incorporation of TMSP additive, which is also consist with the results obtained from EIS experiments, as discussed below. In addition, the $LiNi_{0.5}Mn_{1.5}O_4$ electrode with TMSP containing electrolyte presents better reversible redox peaks corresponding to the valence changes of transition metals [24].

Table 1
Concentration of Mn and Ni that deposit on the lithium electrode with and without TMSP.

	Mn/ppm	Ni/ppm
STD	1.584	0.3762
STD + 1% TMSP	0.3155	0.0199

Table 2
Element concentrations of fresh and cycled $LiNi_{0.5}Mn_{1.5}O_4$ electrodes with and without.

Element	C 1s (%)	O 1s (%)	F 1s (%)	P 2p (%)	Ni 2p (%)	Mn 2p (%)
Fresh	49.1	24.1	14.9		3.6	8.3
STD	39.1	34.9	20.5	4.0		1.5
STD + 1.0% TMSP	46.2	26.9	22.0	2.7		2.2

To further confirm that with the introduction of TMSP into the electrolyte facilitates faster kinetics of the $LiNi_{0.5}Mn_{1.5}O_4$ electrode, rate performance of the high voltage material is carried out. Fig. 4 shows the rate performance of the Li/$LiNi_{0.5}Mn_{1.5}O_4$ cells with and without TMSP-containing. It can be observed that the cells with TMSP-containing shows better rate performance than the cells with baseline electrolyte, especially at 5 C and 10 C discharge rate, the discharge capacity of the cells with additive is 117.2 mAh g^{-1} and 109 mAh g^{-1}, respectively; while 113.7 mAh g^{-1} and 100.9 mAh g^{-1} for the cell without additive, suggesting that the incorporation of TMSP can enhance the kinetics of $LiNi_{0.5}Mn_{1.5}O_4$ electrode, which is consistent with the result of the CV experiments.

The potentiostatic profiles are performed with composite $LiNi_{0.5}Mn_{1.5}O_4$ electrode by using Li/$LiNi_{0.5}Mn_{1.5}O_4$ half cells holding at 5.2 V, vs. Li/Li^+. To minimize the deviation of current floating caused by different loading mass of the composite electrode, the absolute current value was converted to current g^{-1}, as shown in Fig. 5. The Li/$LiNi_{0.5}Mn_{1.5}O_4$ cells with or without TMSP electrolyte were charged to 5.2 V at a constant current of 0.5 C, followed by a constant voltage of 5.2 V for 20 h. The oxidation residual current for the electrolyte with TMSP containing electrolyte on $LiNi_{0.5}Mn_{1.5}O_4$ electrode is lower than that of the baseline (STD) electrolyte, suggesting that incorporation of TMSP can inhibit the oxidative decomposition of electrolyte at 5.2 V, which is most likely due to the more stable surface layer formed on the $LiNi_{0.5}Mn_{1.5}O_4$ electrode in the TMSP added electrolyte.

Electrochemical impedance spectroscopy (EIS) technique was adopted to study the interfacial impedance changes of the Li/$LiNi_{0.5}Mn_{1.5}O_4$ cells upon cycling at high voltage. Fig. 6a and b shows the interfacial impedance changes of the 10th cycle and 200th of the cells with and without TMSP. As we can see from Fig. 6 that the impedance of the surface layer is very similar, 118 and 153 Ω for the cell with STD electrolyte and with TMSP added electrolyte after 10 cycles at room temperature, respectively; however, the impedance of the surface layer grew significantly for the cell with STD after 200 cycles, from 118 to 314 Ω; while the growth of impedance is negligible for the cell with TMSP containing electrolyte after 200 cycles as depicted in Fig. 6b. The EIS results are very consistent with the superior rate performance achieved for the cells with TMSP added as discussed above, suggesting that the surface layer formed on $LiNi_{0.5}Mn_{1.5}O_4$ is more stable and conductive in TMSP added electrolyte, which thus inhibit the continuous electrolyte decomposition upon prolonged cycling at high voltage.

The thermal gravimetric analysis (TGA) of the fresh and the cycled $LiNi_{0.5}Mn_{1.5}O_4$ electrodes in the electrolyte with and without TMSP were analyzed on a TGA instrument with temperature ramp from room temperature to 600 °C, at a heating rate of 10 °C min^{-1} in the nitrogen atmosphere. Fig. 7 shows significant difference of the fresh and the cycled $LiNi_{0.5}Mn_{1.5}O_4$ electrodes in the electrolyte with and without TMSP, the weight loss is 0.9%, 2.3% and 4.4%, respectively. This indicates that the surface of the $LiNi_{0.5}Mn_{1.5}O_4$ electrode without TMSP has more volatile components than that with TMSP containing electrolyte, suggesting that the surface layer on the $LiNi_{0.5}Mn_{1.5}O_4$ electrode cycled without TMSP added

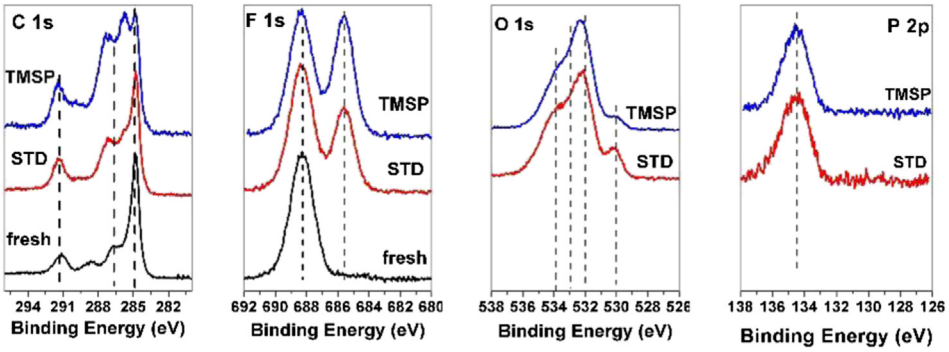

Fig. 10. XPS patterns of the fresh and cycled $LiNi_{0.5}Mn_{1.5}O_4$ electrodes with and without TMSP.

electrolyte consists of more organic species, which is in good agreement with the EIS results as discussed above.

Fig. 8 shows the morphologies of the fresh and the cycled $LiNi_{0.5}Mn_{1.5}O_4$ electrodes in the electrolyte with and without TMSP. Distinct difference was observed of the electrode cycled in baseline electrolyte and the TMSP containing electrolyte. Obviously, more degradation species were precipitated on the bulk particles for the electrode cycled in STD electrolyte, as shown in Fig. 8b. On the other hand, the disintegration of primary $LiNi_{0.5}Mn_{1.5}O_4$ particles was observed after 200 cycles of the cell in the STD electrolyte, while the structure of bulk particles were maintained well in TMSP added electrolyte, as presented in Fig. 8c. Structure changes of the cycled electrodes in baseline electrolyte and TMSP containing electrolyte were further conducted with XRD.

The XRD patterns of the fresh electrode, and the cycled electrodes are provided in Fig. 9a. As we can see that both the cycled $LiNi_{0.5}Mn_{1.5}O_4$ electrodes with and without TMSP have weaker diffraction peaks than the fresh electrode, especially the diffraction peaks 400 and 511 (Fig. 9b). The cycled electrode without TMSP added electrolyte showed dramatically decreased intensities of all the diffraction peaks, but also shifted to higher angles, indicating that the decrease of intensity and lattice parameter of the $LiNi_{0.5}Mn_{1.5}O_4$ electrode without TMSP [25]. But there is no evident of diffraction peaks shift of the cycled $LiNi_{0.5}Mn_{1.5}O_4$ electrode with TMSP containing. The diffraction peaks shift for the electrode cycled in STD electrolyte is most likely caused by the dissolution of Mn^{3+} from the bulk structure [26,27], which leads to the shrinkage of the crystal lattices due to the generation of larger radius of Mn^{2+} via the disproportionation reaction. However, no diffraction peaks shifts are observed for the $LiNi_{0.5}Mn_{1.5}O_4$ electrode cycled in TMSP containing electrolyte, which demonstrates that the dissolution of Mn^{3+} is dramatically inhibited with the incorporation of TMSP additive. This inhibition of Mn dissolution is ascribed to the more stable surface layer formed on the $LiNi_{0.5}Mn_{1.5}O_4$ electrode with the incorporation of TMSP in the surface film formation, which is further confirmed by the ICP-MS and TEM data.

The cycled lithium metallic electrodes with and without TMSP containing were analyzed with ICP-MS. Both of the two lithium electrodes were first washed with DMC for three time, and dissolved in 2% HNO_3 solution, followed by adjust the PH to 7 by adding deionized water to 25 ml. As shown in Table 1, the concentration of Mn and Ni is 1.584 and 0.3762 ppm for the electrolyte without TMSP while 0.3155 and 0.0199 ppm for the electrolyte with TMSP containing, respectively. Combination of the results obtained

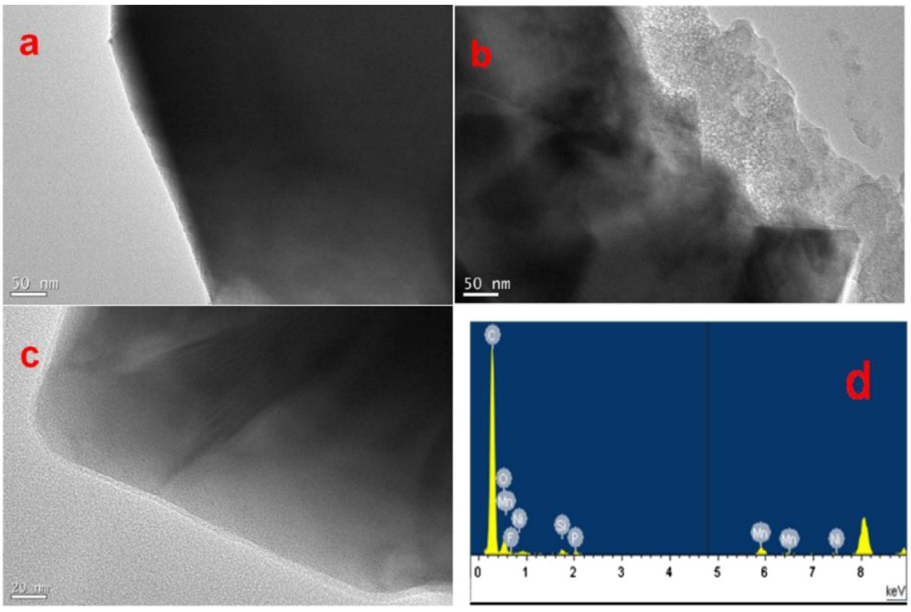

Fig. 11. TEM images of the fresh (a) and cycled $LiNi_{0.5}Mn_{1.5}O_4$ electrodes without (b) and with TMSP (c), the EDX of the $LiNi_{0.5}Mn_{1.5}O_4$ electrode with TMSP containing electrolyte (d).

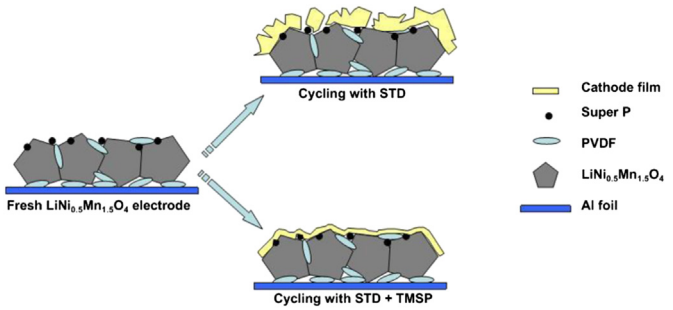

Fig. 12. Schematic illustrations of $LiNi_{0.5}Mn_{1.5}O_4$ electrodes cycling with and without TMSP. TMSP.

from the XRD experiments as discussed above and the ICP-MS results, we believe that the dissolution of Mn is inhibited with the TMSP addition, which enhances the stability of the surface layer. The inhibition of Mn dissolution is believed to be the leading factor to improve the cycling stability of $LiNi_{0.5}Mn_{1.5}O_4$ upon prolonged cycling to high voltage at room temperature or elevated temperature.

To better understand the different surface chemistry on the $LiNi_{0.5}Mn_{1.5}O_4$ electrode with STD and TMSP containing electrolyte, XPS was employed to conduct the components of the surface. Table 2 contains the elemental concentrations of the fresh $LiNi_{0.5}Mn_{1.5}O_4$ electrode, cycled electrodes with STD and TMSP containing electrolyte. After cycling, the concentrations of C, Mn, and Ni are decreased; while the concentrations of O, F, and P are increased, suggesting the formation of a surface film composed of electrolyte decomposition species covering the binder and metal oxide.

The XPS elements spectra are provided in Fig. 10. The C1s spectrum of the fresh $LiNi0_{.5}Mn_{1.5}O_4$ electrode contains three major peaks. The peak at 284.3 eV is assigned to the conductive carbon, and the peaks at 285.7 and 290.4 eV are characteristic of the PVDF binder, which is also characteristic in F 1s spectrum, 687.6 eV. The O 1s spectrum of fresh $LiNi_{0.5}Mn_{1.5}O_4$ electrode is predominant by metal oxide (~529 eV), and consists of low amount of Li_2CO_3 (531.5 eV), which is typically present on fresh cathode electrodes [28].

Analysis of the $LiNi_{0.5}Mn_{1.5}O_4$ cathode electrode cycled in STD and TMSP containing electrolyte reveals the presence of new species in C 1s, O 1s, F 1s, and P 2p spectra corresponding to the electrolyte decomposition products on the electrode surface. After cycling in STD electrolyte, additional peaks are present on the cycled electrodes. C–O (286.5 eV) and C=O (288.5 eV) containing species are observed in C 1s spectra for the electrodes cycled with STD and TMSP containing electrolyte consistent with the presence of lithium alkyl carbonates and polycarbonates [1,9,26]. The correlated peaks for C=O (532–533 eV) and C–O (533–534 eV) containing species are observed in the O 1s spectra. The intensities of C 1s peaks for the electrode cycled in TMSP containing electrolyte are stronger than those of C 1s peaks for the electrode cycled in STD electrolyte; correlatively, the intensities of O 1s peaks for the electrode cycled in TMSP containing electrolyte are weaker than those of the peaks for the electrode cycled in STD electrolyte, suggesting more C-based decomposition products present on the $LiNi_{0.5}Mn_{1.5}O_4$ electrode cycled in TMSP containing electrolyte; while more O-containing species are present on the electrode cycled in STD electrolyte, which is consistent with the EIS data. In addition, peaks characteristic of LiF (685 eV, F 1s) and $Li_xPO_yF_z$ (686–687 eV F 1s, ~134 eV, P 2p) are observed, although the F 1s peak of PVDF binder overlaps with the F 1s peak for $Li_xPO_yF_z$. Furthermore, the peak of metal oxide (~529 eV) is still visible, suggesting the surface layer is thin.

TEM images of fresh $LiNi_{0.5}Mn_{1.5}O_4$ electrode and the cycled electrode are shown in Fig. 11. The surface of fresh $LiNi_{0.5}Mn_{1.5}O_4$ electrode is clean and smooth, as shown in Fig. 11a. After cycling at high voltage without TMSP (Fig. 11b), the $LiNi_{0.5}Mn_{1.5}O_4$ particles have been corroded and converted to a porous structure, which is consistent with Mn and Ni dissolution as we discussed above. Besides, a surface layer was observed on the edge of the particle, and its thickness is ranging from 100 to 150 nm. As regards to the electrode cycled in TMSP containing electrolyte, the edges of the electrodes maintained very well, a very thin and uniform film with 4 nm thickness is observed, Fig. 11c. EDX of the cycled electrode in TMSP containing electrolyte is provided in Fig. 11d, C, O, F, and P is detected on surface corresponding to the electrolyte decomposition. In addition, Si is observed on the surface as well, which further confirmed that TMSP participates the surface layer formation and thus changed the chemistry and structure of the surface layer on $LiNi_{0.5}Mn_{1.5}O_4$ electrode upon cycling at high voltage. The enhanced cycling performance with the TMSP added electrolyte is mostly ascribed to the changes of chemistry and structure of the surface layer with the TMSP participation.

Fig. 12 shows a schematic of $LiNi_{0.5}Mn_{1.5}O_4$ electrode with and without TMSP after cycling. The cathode film on the $LiNi_{0.5}Mn_{1.5}O_4$ electrode is thick and loose, while it is compact and thin for the $LiNi_{0.5}Mn_{1.5}O_4$ electrode with TMSP, which prevents the decomposition of electrolyte on the cathode at high voltage and protects the $LiNi_{0.5}Mn_{1.5}O_4$ electrode by suppressing the Mn and Ni dissolution from the $LiNi_{0.5}Mn_{1.5}O_4$ electrodes.

4. Conclusions

The cycling performance of $Li/LiNi_{0.5}Mn_{1.5}O_4$ cells with 1.0 M $LiPF_6$ in EC/DMC (1/2, v/v) with and without tris (trimethylsilyl) phosphate (TMSP) has been investigated. The incorporation of TMSP into the electrolyte can dramatically increase the cycling performance of $Li/LiNi_{0.5}Mn_{1.5}O_4$ cell at high voltage and elevated temperature. Electrochemical methods and ex-situ analysis of the $LiNi_{0.5}Mn_{1.5}O_4$ electrode were conducted via a combination of CV, EIS, XPS, XRD, SEM, TEM with EDX, TGA, and ICP-MS to better understand of the roles of the additive in capacity retention upon cycling at high voltage. Incorporation of TMSP results in generation of a more stable and more conductive surface film on $LiNi_{0.5}Mn_{1.5}O_4$ electrode surface, which inhibits the decomposition of electrolyte and depresses the dissolution of Mn upon cycling at high voltage and elevated temperature. The inhibition of electrolyte decomposition and Mn dissolution play a predominant role to enhance the cycling performance of $Li/LiNi_{0.5}Mn_{1.5}O_4$ cell upon cycling at high voltage, 4.9 V vs. Li/Li^+.

Acknowledgments

This research work is supported by the National Natural Science Foundation of China (21003054, 21373092, 21273084, 21303051), the Joint Project of National Natural Science Foundation of China and Natural Science Foundation of Guangdong (No. U1134002), Natural Science Foundation of Guangdong Province (10351063101000001), Specialized Research Fund for the Doctoral Program of Higher Education (20104407120008).

References

[1] L. Yang, B. Ravdel, B.L. Lucht, Electrochem. Solid-State Lett. 13 (2010) A95–A97.
[2] G.Q. Liu, L. Wen, Y.M. Liu, J. Solid State Electrochem. 14 (2012) 2191–2202.

[3] R. Santhanam, B. Rambabu, J. Power Sources 195 (2010) 5442–5451.
[4] J.H. Cho, J.H. Park, M. Hee, H.K. Song, S.Y. Lee, Energy Environ. Sci. 5 (2012) 7124.
[5] E.G. Leggesse, J.C. Jiang, J. Phys. Chem. A 116 (2012) 11025.
[6] H.B. Kang, S.T. Myung, K. Amine, S.M. Lee, Y.K. Sun, J. Power Sources 195 (2010) 2023.
[7] Y. Watanabe, S.I. Kinoshita, S. Wada, K. Hoshino, H. Morimoto, S.I. Tobishima, J. Power Sources 179 (2008) 770.
[8] Y.K. Han, J. Jung, S. Yu, H. Lee, J. Power Sources 187 (2009) 581.
[9] D. Lu, M. Xu, L. Zhou, A. Garsuch, B.L. Lucht, J. Electrochem. Soc. 160 (5) (2013) A3138–A3143.
[10] S.W. Kim, V.G. Kumar, D.H. Seo, Y.U. Park, J. Kim, H. Kim, J. Kim, J. Hong, K. Kang, Electron. Mater. Lett. 7 (2011) 105–108.
[11] J. Liu, A. Manthiram, Chem. Mater. 21 (2009) 1695.
[12] R. Alcantara, M. Jaraba, P. Lavela, J.L. Tirado, Electrochim. Acta 47 (2002) 1829.
[13] Y.K. Sun, Y.S. Lee, M. Yoshio, K. Amine, Electrochem. Solid-State Lett. 5 (2002) A99.
[14] H.M. Wu, I. Belharouak, A. Abouimrane, Y.K. Sun, K. Amine, J. Power Sources 195 (2010) 2909.
[15] K. Xu, B. Deveney, K. Nechev, Y. Lam, T.R. Jow, J. Electrochem. Soc. 155 (2008) A959–A964.
[16] A. Abouimrane, Belharouak, K. Amine, Electrochem. Commun. 11 (2009) 1073–1076.
[17] K. Xu, C.A. Angell, J. Electrochem. Soc. 149 (2002) A920–A926.
[18] K. Xu, Chem. Rev. 104 (2004) 4303.
[19] S. Dalavi, M. Xu, B. Knight, B.L. Lucht, Electrochem. Solid-State Lett. 15 (2) (2012) A28–A31.
[20] M. Xu, Y. Liu, B. Li, W. Li, X. Li, S. Hu, Electrochem. Commun. 18 (2012) 123–126.
[21] Jie Zhang, Jiulin Wang, Jun Yang, Yanna NuLi, Electrochim. Acta 117 (2014) 99–104.
[22] Guochun Yan, Xinhai Li, Zhixing Wang, Huajun Guo, Chao Wang, J. Power Sources 248 (2014) 1306–1311.
[23] L. Yu, Y. Cao, H. Yang, X. Ai, J. Solid State Electrochem. 10 (2006) 283–287.
[24] H.G. Jung, M.W. Jang, J. Hassoun, Y.K. Sun, B. Scrosati, Nat. Commun. 2 (2011) 516.
[25] Y.J. Liu, X.H. Li, H.J. Guo, Z.X. Wang, Q.Y. Hu, W.J. Peng, Y. Yang, J. Power Sources 189 (2009) 721.
[26] G.G. Amatucci, C.N. Schmutz, A. Blyr, C. Sigala, A.S. Gozdz, D. Larcher, J.M. Tarascon, J. Power Sources 69 (1997) 11.
[27] S. Komaba, N. Kumagai, T. Sasaki, Y. Miki, Electrochemistry 69 (2001) 784.
[28] W. Li, B.L. Lucht, J. Electrochem. Soc. 153 (2006) A1617.